

MTL TR 92-71

AD-A258 931



ASSESSMENT OF HELICOPTER COMPONENT STATISTICAL RELIABILITY COMPUTATIONS

WILLIAM T. MATTHEWS and DONALD M. NEAL
MECHANICS AND STRUCTURES BRANCH

September 1992

DTIC
SELECTE
DEC 04 1992
S B D

Approved for public release; distribution unlimited.

92 12 02 026



US ARMY
LABORATORY COMMAND
MATERIALS TECHNOLOGY LABORATORY



92-30782



U.S. ARMY MATERIALS TECHNOLOGY LABORATORY
Watertown, Massachusetts 02172-0001

The findings in this report are not to be construed as an official Department of the Army position, unless so designated by other authorized documents.

Mention of any trade names or manufacturers in this report shall not be construed as advertising nor as an official indorsement or approval of such products or companies by the United States Government.

DISPOSITION INSTRUCTIONS

Destroy this report when it is no longer needed.
Do not return it to the originator.

UNCLASSIFIED

SECURITY CLASSIFICATION OF THIS PAGE (When Data Entered)

REPORT DOCUMENTATION PAGE		READ INSTRUCTIONS BEFORE COMPLETING FORM
1. REPORT NUMBER MTL TR 92-71	2. GOVT ACCESSION NO.	3. RECIPIENT'S CATALOG NUMBER
4. TITLE (and Subtitle) ASSESSMENT OF HELICOPTER COMPONENT STATISTICAL RELIABILITY COMPUTATIONS		5. TYPE OF REPORT & PERIOD COVERED Final Report
7. AUTHOR(s) William T. Matthews and Donald M. Neal		6. PERFORMING ORG. REPORT NUMBER
9. PERFORMING ORGANIZATION NAME AND ADDRESS U.S. Army Materials Technology Laboratory Watertown, Massachusetts 02172-0001 SLCMT-MRS		8. CONTRACT OR GRANT NUMBER(s)
11. CONTROLLING OFFICE NAME AND ADDRESS U.S. Army Laboratory Command 2800 Powder Mill Road Adelphi, MD 20783-1145		10. PROGRAM ELEMENT, PROJECT, TASK AREA & WORK UNIT NUMBERS D/A Project 61202.H84
14. MONITORING AGENCY NAME & ADDRESS (if different from Controlling Office)		12. REPORT DATE September 1992
		13. NUMBER OF PAGES
		15. SECURITY CLASS. (of this report) Unclassified
		15a. DECLASSIFICATION/DOWNGRADING SCHEDULE
16. DISTRIBUTION STATEMENT (of this Report) Approved for public release; distribution unlimited.		
17. DISTRIBUTION STATEMENT (of the abstract entered in Block 20, if different from Report)		
18. SUPPLEMENTARY NOTES		
19. KEY WORDS (Continue on reverse side if necessary and identify by block number) Reliability Probability density function Fatigue life Probability Flight loads Helicopter		
20. ABSTRACT (Continue on reverse side if necessary and identify by block number) (SEE REVERSE SIDE)		

Block No. 20**ABSTRACT**

This report identifies potential errors in computing high statistical reliability for a required component fatigue life. The reliability values were determined from application of a joint probability density (JPD) analysis used in an American Helicopter Society round robin safe life problem.

In the analysis normal probability density functions (PDFs) were assumed for both the material strength and the spectrum load values. The PDF model parameters were varied and the PDFs were slightly modified (contaminated) in order to examine the sensitivity in computing high statistical reliability when uncertainties exist in assuming the PDF. Lower tails of the PDFs were also modified by truncation, independent of the model contamination, in order to determine the relative influence on reliability from tail modifications as compared with the parameter uncertainties and contamination. The stability of statistical estimates of the extreme tail quantiles and their corresponding probabilities as a function of sample size were examined for a generic distribution.

Assuming a PDF to represent load or material strength is a substantially more critical issue than accurate representation of the extreme lower tail of the PDF when computing high reliability. Sampling trials for extreme tail quantiles and reliabilities indicate that unstable values can result from sample sizes of 100.

The primary conclusion from these analytic results is that the computation of a high statistical reliability may have little or no association with actual engineering high reliability.

CONTENTS

	Page
INTRODUCTION	1
FATIGUE LIFE COMPUTATIONS	2
RELIABILITY AS A FUNCTION OF LIFE	3
CONTAMINATED PROBABILITY DENSITY FUNCTIONS	4
MODIFYING TAILS OF THE PDFS	5
PDF PROBABILITY AT TRUNCATION POINTS	6
RESULTS AND DISCUSSION	7
CONCLUSIONS	10
REFERENCES	11
TABLES AND FIGURES	12

DTIC QUALITY INSPECTED 1

Accession For	
NTIS GRA&I	<input checked="" type="checkbox"/>
DTIC TAB	<input type="checkbox"/>
Unannounced	<input type="checkbox"/>
Justification	
By	
Distribution/	
Availability Codes	
Dist	Avail and/or Special
A-1	

INTRODUCTION

The use of a quantitative high reliability requirement for a helicopter component fatigue design has received considerable attention recently. The U. S. Army established a requirement of .999999 ("six nines") reliability for dynamic components in its most recent helicopter development¹. Subsequently, the American Helicopter Society Subcommittee on Fatigue and Damage Tolerance, conducted a round robin study of high reliability fatigue methodology applied to a simple structural element². A review of the round robin³ noted difficulties in the reliability analysis. Each participant used a different fatigue curve and fatigue limit variability which resulted in significantly different fatigue lives, for the six nines reliability requirement. A recent fatigue analysis by a helicopter manufacturer⁴ found that "reliability is very sensitive to changes in the population mean strength and scatter". In addition Reference 4 notes "the conclusions of this study are not fully applicable to actual fleet management due to the presence of statistically indeterminate variables such as degraded or non-conforming components".

The present authors in previous study, have investigated the sensitivity of high reliability computations from a stress-strength model⁵ to uncertainties in the identification of the probability density functions(PDFs) in the model. The uncertainties are associated with the selection of competing parametric forms(e.g, normal, log-normal, Weibull, etc.) or with the undetected presence of contaminated populations. Contaminated distributions could be bimodal, caused by degraded or non-conforming components, or could be the result of by unexpected loading anomalies. The results from Reference 5 showed that high reliability estimates can vary substantially even for "almost undetectable" differences in the assumed stress and strength PDFs. The authors have also investigated the sensitivity of safe life fatigue reliability of a simple structural element loaded by a simplified spectrum to a variety of uncertainties⁶, demonstrating that a small amount of uncertainty in the parameters of the load or strength PDF resulted in a substantial reduction in the high statistical reliability values for a specified lifetime of the component.

The round robin review, Reference 3, also expressed a concern for the effect of inaccuracies or truncations of the tails of the distributions. An investigation of the truncation of known normal PDF was proposed in order to determine an "acceptable degree of truncation" in computing high statistical reliability. Apparently, this determination would be expected to indicate the portion of the tail region in which an accurate representation of the PDF is not required.

In this report the AHS round robin fatigue problem and its methodology, Reference 2, will be used to investigate the cited issues by considering: a) The effect of small changes in the PDF parameters on the reliability-life relationship. b) The influence upon reliability of the consideration of PDFs which are contaminated, using the methods of Reference 5, by bimodal effects. c) The "true" reliability associated with fatigue lives which have been obtained by satisfying an "apparent" six nines reliability based on normal PDFs which have been truncated in the extreme tail region. d) The relative influence on high statistical reliability of parameter uncertainties, contamination and truncations of the PDF. The consideration of issues involving the extreme tails of the PDFs requires an accurate measure of the truncation point locations, which is difficult to achieve, since sufficient amounts of data is usually not available. In practice, truncation point locations would be estimated from small data sets of load or strength measurements. The stability of the statistical

estimates of the extreme tail quantile and probability values will be investigated based on sampling simulations of a generic normal PDF.

These results will be assessed to indicate the potential role of the PDF tail truncation analysis in providing conclusive information on the acceptability of PDF modeling and whether a quantified .96 reliability provides a meaningful measure which correlates with levels of structural integrity.

FATIGUE LIFE COMPUTATIONS

The following standardized fatigue life computation procedures were obtained from a round robin study conducted by the AHS, Reference 2. The form of the S-N curve is,

$$N = C(S^* - S_E)^D, \quad (1)$$

where N = number cycles to failure; S_E = fatigue strength for very large N values, for minimum stress equal to zero; S^* = effective maximum cyclic stress, for minimum stress equal to zero, equivalent to spectrum stresses; C and D are parameters from regression least squares analysis.

In order to apply the S-N curve in Equation 1 using the actual operating load spectrum, the following relation for S^* is required:

$$S^* = \frac{\alpha \cdot S_u \cdot S_L}{S_u - \alpha \cdot S_m + \alpha \cdot S_L/2}. \quad (2)$$

This equation represents a form of the Goodman correction factor used in Reference 2, which converts a defined spectrum mean stress and stress range to an equivalent stress range which causes equal fatigue damage from zero to specified S^* value. S_u represents the ultimate strength of the material. S_m and S_L represent the mean and range respectively of the nominal stress from a rainflow count obtained in Reference 2, of the standardized Felix 28 spectrum as tabulated in Table 1. The α value is a scaling parameter for the spectrum load values S_L and S_m representing the effective load scaling, over the lifetime of a component. This parameter can provide changes in the baseline spectrum load in order to account for differences in usage, pilot technique, weather, weight, etc.

Let the fatigue life N_p represent the number of passes prior to the component failure. Then from Miner's Rule, Reference 6,

$$N_p = 1/DF \quad (3)$$

where,

$$DF = \sum_{k=1}^{NK} \frac{n(k)}{N(k)}. \quad (4)$$

The $n(k)$ s represent the number of cycles for a specific k value and NK represents the total number of spectrum load values from Table 1. The $N(k)$ s are the results from Equation 1.

RELIABILITY AS A FUNCTION OF LIFE

The following procedures suggested in Reference 1, were applied in order to obtain high reliability(R) estimates at a specified lifetime. In the analysis the unreliability \bar{R} is initially determined from application of a discrete joint probability density(JPD) function. The function provides probabilities associated with the simultaneous occurrence of both a spectrum load and a material strength value. In the analysis both the spectrum load scaling factor α and the material fatigue strength s , where the mean $\mu_s = S_E$, are represented by a normal PDFs as shown in Figure 1. This representation allows for application of the JPD analysis in addition to providing for potential variability in loading and material strength. The scaled version of the spectrum load (αS_L) is only involved in computing N in Equation 1 but not the \bar{R} estimate. The \bar{R} computation involving only α and s in the JPD computation is therefore simplified. Substitution of α for αS_L is valid since both are normally distributed and their probability computations are independent of location. That is, the scaled and unscaled version of the load will provide identical probability estimates with respect to the JPD computation. Since the "event", of identifying a particular value of α with a component, is independent of the "event" of using a component with particular fatigue strength, the joint probability that $\alpha = \alpha_i$ and $s = s_j$ occurs simultaneously can be written as,

$$P(\alpha = \alpha_i, s = s_j) = P(\alpha = \alpha_i) \cdot P(s = s_j), \quad (5)$$

where $i = 1, 2, 3, \dots, n_1$ and $j = 1, 2, 3, \dots, n_2$. The n_1 and n_2 represent the number of events for load and strength respectively. The regions A_α and A_s where the events occur which produce higher probability of failure are bounded by the normal PDFs as shown in Figure 1. The load and strength functions are,

$$f_\alpha(\alpha) = \frac{1}{\sigma_\alpha \sqrt{2\pi}} e^{-\frac{1}{2} \left(\frac{\alpha - \mu_\alpha}{\sigma_\alpha} \right)^2}, \quad (6)$$

and

$$f_s(s) = \frac{1}{\sigma_s \sqrt{2\pi}} e^{-\frac{1}{2} \left(\frac{s - \mu_s}{\sigma_s} \right)^2}, \quad (7)$$

where $(\mu_\alpha, \sigma_\alpha)$ and (μ_s, σ_s) are the population means and standard deviations for the load and strength, respectively. Referring to Figure 1 and Equation 5, the JPD can be written as

$$P_{i,j} = P_{\alpha_i} \cdot P_{s_j}, \quad (8)$$

where,

$$P_{\alpha_i} = \Delta\alpha_i \cdot f_\alpha(\bar{\alpha}_i), \quad (9)$$

$$P_{s_j} = \Delta s_j \cdot f_s(\bar{s}_j), \quad (10)$$

and $i = 1, 2, 3, \dots, n_1$ and $j = 1, 2, 3, \dots, n_2$. After determining the joint probability values $P_{i,j}$ from Equation 8, the corresponding α and s associated with these probabilities are introduced in Equations 2 and 1 respectively. This determines a specific number ($N_{i,j}$) cycles to failure of the material for the corresponding probability ($P_{i,j}$) of the joint occurrence of α_i and s_j . The lifetime estimate N_P from Equation 3 for the joint α_i and s_j event is obtained from the following application of the spectrum load data $\{S_L(k)\}_1^{NK}$, $\{S_m(k)\}_1^{NK}$ and $\{n(k)\}_1^{NK}$ in Table 1, where NK is the number

of spectrum loads. The damage fraction for a specified event can be determined from Equation 4 and written as

$$DF_{ij} = \sum_{k=1}^{NK} \frac{n(k)}{N_{ij}(k)} \quad (11)$$

where $n(k)$ s are the spectrum load cycles corresponding to the original tabulated loads $S_L(k)$. From Equations 3 and 8, the lifetime values are then computed from

$$N_P(ij) = 1/DF_{ij} \quad (12)$$

These values correspond to the joint probability that $\alpha = \alpha_i$ and $s = s_j$. The above process is repeated $M = n_1 n_2$ times, where n_1 and n_2 represent the number of mesh points associated with the tail region of the PDFs in Figure 1. All combinations of i and j are introduced in order to obtain paired P_{ij} and $N_P(ij)$ values. Ordering only the N_P values from the smallest to largest and retaining their original corresponding P_{ij} probabilities describes a discrete PDF representing the component probability of failure $P_f(t)$ as an array of lifetimes $\{N_P^*(t)\}_1^M$, where t is an integer defining the ordering of the N_P^* values. See a graphical display of a PDF in Figure 2. In order to obtain the unreliability \bar{R} for a given t_1 in Figure 2, a cumulative density computation is required. This is accomplished by selecting an ordered value from N_P^* and computing the sum

$$\bar{R}(t_1) = \sum_{t=1}^{t_1} P_f(t) \quad (13)$$

Note, the reliability R can be obtained from $R = 1 - \bar{R}$ and the lifetime values can be determined from a given \bar{R} .

CONTAMINATED PROBABILITY DENSITY FUNCTIONS

In order to illustrate the sensitivity of high reliability calculations to small deviations from the assumed models, the approach taken in Reference 5, is applied. Consider the situation where with a high probability of $1 - \epsilon$, samples are obtained from a primary PDF, while with probability ϵ samples come from a secondary PDF. This bimodal probability model is a type of a general class referred to as a *contaminated* models. The secondary component is called the *contamination* and the probability ϵ is the *amount* of contamination. An example may help clarify this idea. Consider the situation where 99% of the specimens are obtained from a population of "good" specimens while the remaining 1% of the time consistently lower strength measurements are obtained, either due to manufacturing defects or to faulty testing. The primary PDF would correspond to the "good" specimens, the contamination would represent the distribution of flawed specimens, and the amount of contamination is $\epsilon = 0.01$. The following procedure is introduced in order to examine the effects of computing high reliability values when uncertainties exist in selecting the PDFs for the joint density computations. Initially, values are obtained from the JPD computation using PDFs f_α and f_s in Equations 6 and 7. Another R value is then obtained by applying the PDFs with a small amount of contamination ϵ .

The f_s PDF with variance contamination for the strength data is written as,

$$f_{cs}^v = (1 - \epsilon)f_s(\mu_s, \sigma_s^2) + \epsilon f_s(\mu_s, k_1^2 \sigma_s^2), \quad (14)$$

where μ_s and σ_s are defined in Equation 7, k_1 is a scaling factor and 100ϵ is the percent contamination. A similar contaminated distribution for f_α representing load α can be written as

$$f_{\alpha}^v = (1 - \epsilon)f_\alpha(\mu_\alpha, \sigma_\alpha^2) + \epsilon f_\alpha(\mu_\alpha, k_1^2 \sigma_\alpha^2), \quad (15)$$

with scaling factor k_1 and μ_α and σ_α obtained from Equation 6. Variance contamination produces effects which can be considered to represent uncertainties associated with the selection of competing PDF models.

A strength distribution with mean location contamination is

$$f_s^L = (1 - \epsilon)f_s(\mu_s, \sigma_s^2) + \epsilon f_s(\mu_s \pm k_2 \sigma_s, \sigma_s^2), \quad (16)$$

where k_2 is a scaling factor for μ_s and the sign determines which tail of the function is to be contaminated and σ_s^2 is the variance for $\mu_s \pm k_2 \sigma_s$. The contaminated function for load α can be determined in a similar manner. The location contaminated PDF can represent the rare occurrence of exceptionally high loads or the unusually low material strength of a degraded or non-conforming component in computing the reliability. For $\epsilon = .01$ and $k_1 = 4$, graphical results in Figure 3, show an almost undetectable difference between the original normal PDF and the contaminated one. A linear relationship to obtain R from the JPD function application can be obtained by combining both contaminated and uncontaminated functions such that,

$$R^* = (1 - \epsilon_1)(1 - \epsilon_2)R_{00} + \epsilon_1(1 - \epsilon_2)R_{10} + \epsilon_2(1 - \epsilon_1)R_{01} + \epsilon_2\epsilon_1R_{11}, \quad (17)$$

where $100\epsilon_1$ and $100\epsilon_2$ are the percent contamination in the α and s distributions and R_{mn} represents reliabilities obtained from contaminated conditions designated by m and n . If $m, n = 0$, then there is no contamination. If $m = 1$ and $n = 0$ then f_α is contaminated. If $m, n = 1$, then both f_α and f_s are contaminated. For example, if there is contamination of the strength PDF with respect to the variance then,

$$R^* = (1 - \epsilon_2)R_{00} + \epsilon_2R_{01}. \quad (18)$$

The R_{mn} values are obtained from \bar{R} in Equation 13. This procedure provides an effective approach for demonstrating the effects of PDF uncertainties in determining high R values.

MODIFYING TAILS OF THE PDFS

A modification of the f_α and f_s PDFs' upper and lower tail regions respectively was introduced in the analysis to investigate truncation effects as suggested in Reference 3. A proposed modification⁷ is shown in Figure 4. The lumping method of truncation shown in the figure was selected so that the area under the modified PDF remains equal to one. This was accomplished by determining the area under extreme tail regions associated with the probabilities $P_{\alpha n_1}$ and $P_{s n_2}$ obtained from Equations 20 and 21. These areas were lumped at the truncation points z_1 and z_2 for α and s and the reliability R_L values were determined from Equation 13, with the lumped f_α , f_s . A comparison was then made between lumped and unlumped results in order to determine if the effects of the uncertainties in the extreme tails are significant in computing high R values. The modification also represents a substantial difference in the lower tail region when compared with the original PDFs.

The R computation using the lumped PDFs, in Figure 4, is the same as that described previously, except in Equation 8,

$$P_{n_1 n_2} = P_{\alpha_{n_1}} \cdot P_{s_{n_2}}, \quad (19)$$

where,

$$P_{\alpha_{n_1}} = \int_{z_1}^{\infty} f_{\alpha} \cdot d\alpha, \quad (20)$$

$$P_{s_{n_2}} = \int_{-\infty}^{z_2} f_s \cdot ds, \quad (21)$$

and $z_1 = \mu_{\alpha} + \lambda_1 \sigma_{\alpha}$, $z_2 = \mu_s + \lambda_2 \sigma_s$, are the truncation points of the PDFs shown in Figure 4. The f_{α} and f_s PDFs are defined in Equations 6 and 7. The R computation procedures are then applied using the newly defined $P_{\alpha_{n_1}}$ and $P_{s_{n_2}}$ values.

PDF PROBABILITY AT TRUNCATION POINTS

The lumping procedure described previously was introduced in order to determine the effects on the R values from modifications to the extreme tail of the PDFs.

In applying Equations 20 and 21, it is assumed that the PDFs and the truncation points z_1 and z_2 are known exactly; which is usually not the case for engineering problems involving material strength or loading measurements. Since the accuracy in estimating the truncation point locations is essential in determining the importance of correct extreme tail representation in obtaining high R values, the following study was performed involving determination of the reliability and quantile values at selected truncation points as a function of sample size. Quantile values of f_s can written as,

$$S_q = \mu_s - K \cdot \sigma_s, \quad (22)$$

where μ_s and σ_s are known mean and standard deviation of f_s . The K values can be selected to define points where truncation may be introduced in the high reliability computation. Unfortunately, the μ_s and σ_s values are not known sufficiently well for an accurate measurement of S_q unless very large data sets are applied.

The following simulation process examines the sample size(n_2) effects in computing the truncation points. In the simulation process, a n_2 set of s_i normally distributed values are selected from

$$s_i(i) = \mu_s(1 + v_s \cdot Q_i), i = 1, 2, 3, \dots, n_2 \quad (23)$$

where the Q_i values are obtained from a standard normal distribution with $\mu_s = 100$ and $v_s = .10$. The v_s value is the CV = σ_s/μ_s and μ_s is the population mean. From the s_i values the mean \bar{s}_i and variance $VAR(s_i)$ are determined. An estimate of the population quantile S_q is then

$$\hat{S}_q = \bar{s}_i - K \cdot (VAR(s_i))^{1/2} \quad (24)$$

The probability P_T , where P_T equals $\text{Prob}[s_i \geq S_q]$ can be estimated by the proportion of s_i values which are greater than S_q . The process involving Equations 23 and 24 is repeated many times so that

the P_T and S_q values are not effected by further increasing the number of simulations. The range of P_T and S_q values is a measure of the statistical stability of the sampling process. Particular quantile values such as 1% or 99% can be obtained by forming a cumulative probability distribution for S_q and P_T . The probabilities are ordered from the smallest to largest and their percent is determined from their numbered position in the ordering which is divided by the total number of simulations. The S_q quantile is the value at the same numbered position of interest.

RESULTS AND DISCUSSION

In this section, results are obtained for the AIIS round robin problem in Reference 2. A thin AISI 4340 steel plate with a central hole is loaded by the Felix 28 spectrum. The ASTD S - N curve coefficients are used: $C = 3.5 \times 10^6$, $D = -1.47164$ and $S_E = 54.5\text{KSI}$. The S_U value is 180KSI in Equation 2. The number of mesh points n_1 and n_2 of the PDFs in the JDF computation (Equation 5) are each 50, where $C_\alpha = \mu_\alpha$ and $C_s = \mu_s$ (see Figure 1).

In Figure 5, representation of reliability as a function of life (N_P) is shown for selected CV values used in defining the PDFs f_α and f_s in the R computation, with a mean load factor (μ_α) of .70. The results show a very rapid initial decrease in reliability followed by a more moderate decline in reliability as the lifetime values increase. Results were the same for other μ_α values. R estimates also decreased with an increase in the assumed CV value. For example, a CV = .05 for both PDFs provides a much greater $R(.9_{(11)})$ estimate than for a CV = .07 which is $.9_{(6)}$ when $N_P = 100$. The results designated by the * were obtained from applying lumped PDFs for $\lambda_1 = \lambda_2 = 3.5$. These values of λ are almost the maximum amount of truncations that will provide the $R = .9_6$ requirement. The maximum truncation was avoided because the $R = .9_6$ would be met at the discrete probability value of the discrete joint distribution which includes the lumped values. The $R = .9_6$ value from the lumped PDF differs slightly from the unlumped PDF where $R = .9_{54}$ when $N_P = 50$ and the CV = .8. This result indicates that modifications of the extreme lower tails of the PDFs do not cause large differences in computing high reliability.

Figure 6 shows reliability as a function of life for selected μ_α load factors. As in Figure 5, there is a reduction in reliability with an increase in N_P values. There is also an obvious decrease in reliability with an increase in load factor. In the case where $N_P = 275$, an μ_α of .5 and .6 resulted in $R = .9_{11}$ and $.9_6$ respectively. This shows a substantial sensitivity in computing R for a relatively small differences which may occur in estimating μ_α .

Figure 7 also shows the reliability values as a function of life (N_P). The assumed CV value for the PDFs is .07 and applied loads are $\mu_\alpha = .5$ and .7. The dash lines represent results from applying the contaminated PDFs described in Equations 14 and 15, for the case of 1% contamination in both PDFs and $k_1 = 4$. This almost undetectable level of contamination caused a drastic reduction in reliability for $R > .9_6$. The results from the contaminated PDFs application which represent the uncertainties in assuring a specific function, demonstrate the importance of identifying precise PDFs in computing component high statistical reliability. In contrast, at $N_P = 130$, the unlumped result for of $.9_{52}$ is only moderately reduced from the value of $.9_6$ obtained for lumped PDFs for λ_1

and $\lambda_2 = 3.5$.

In Table 2, reliability results are tabulated using both lumped(R_L) and unlumped(R_{UL}) PDF applications for selected CV values. These results show a reduction in R_L and R_{UL} values with increasing CV values. In the case of CV = .05 and .06, the R_L estimate of .976 was the maximum obtainable because of the discrete nature of the PDF truncation procedures. Comparing the values of $R_L = .976$ with $R_{UL} = .96$ for CV = .07 shows a relatively small difference in the reliability values. This result indicates that uncertainties in modeling the extreme lower and upper tails of the PDFs cause relatively small differences in computing high R values. The issue that is important involves the substantial reduction in the R_L and R_{UL} values with increasing CVs. Since the CV values are often estimated from coupon data that are assumed to be relevant to actual component behavior, substantial uncertainties can result in estimating R.

Table 3 shows effects in computing R from applying both contaminated and uncontaminated PDF applications. In the case where $\mu_\alpha = .5$ and $N_P = 80$, the uncontaminated PDF result is $R \gg .912$. When there is a 1% contamination of PDF for the load, the value is reduced to .96. Contaminating the strength PDF by 1% resulted in a reduction from twelve nines(uncontaminated) to three nines(contaminated) in the R estimate. Very similar results were obtained for contamination of both PDFs. As previously shown in Figure 7, obtaining extremely high reliability greater than twelve nines will not provide the necessary conservative estimate for R if there is even a very small amount of uncertainty in assuming a PDF in the R computation. The case where $\mu_\alpha = .7$ represents application of both the lumped and contaminated PDFs in the R computation. The lumped PDF result without contamination showed $R = .976$ which is reduced to .928955 when the contaminated PDF was also applied. Again, this substantial reduction in R demonstrates the importance in the accuracy of the PDF. Potential uncertainties associated with defining the extreme tails of the PDFs become insignificant relative to the accuracy of PDF assumption in computing high R values. The table also shows that by increasing the CV value the N_P value is reduced but the reduction in R from the contaminated PDF are the same as those for CV = .07. Summarizing the results in the table: it is critical in computing high statistical R values that the PDFs are known almost exactly while uncertainties in the extreme tails of the PDFs are relatively insignificant.

Table 4 provides results similar to those in Table 2 except that the load μ_α is varied in order to examine the effects of uncertainty in determining the mean scaling load factor in the reliability - life estimating process. The results again show a substantial difference in R for an uncertainty in μ_α . For example, when $\mu_\alpha = .7$, $R = .96$ and for $\mu_\alpha = .8$, $R = .93662$ which implies that there will be one failure and 338 failures in a million for loads $\mu_\alpha = .7$ and .8 respectively. This substantial difference relative to uncertainties in estimating μ_α indicates that the R computations are very sensitive to uncertainties in the load. The table shows little difference between R_{UL} and R_L for $\mu_\alpha \geq .7$. When $\mu_\alpha < .7$ no quantitative comparisons are possible because of the PDF truncations. The R value for $\mu_\alpha = .7$ shows a substantial decrease in R_{UL} from approximately .96 to .9289 for the uncontaminated and contaminated PDFs respectively. A similar result is shown for R_L at $\mu_\alpha = .7$. The R_{UL} and R_L results at $\mu_\alpha = .7$ showed a small effect on R with a substantial modification of the extreme tails of PDFs. This shows that the PDF assumption is critical in computing R while accuracy in representing the extreme tail of the PDFs is much less critical.

In Table 5 are the results of sampling a generic normal PDF to examine the stability of the statistical estimates at the potential truncation points. The median probability and quantile values are shown for a range of sample sizes(n_2). Included in the results are the upper and lower bounds on the 98% confidence interval on the median estimates. Reliability(P_T) values are obtained at $K = 3.5$ and 4.75 where truncation may introduced in high reliability computations in studying effects in PDF tail modifications. This was done in order to examine if there is instability in P_T at the points due to the sample size. The sampling trials were repeated 6000 times which was sufficient to ensure that the tabulated values would not change with additional trials. Results from the table indicate that relatively unstable P_T values will be obtained for even a sample size of 100. In this case, the true P_T value is .93767 for $K = 3.5$ but the simulation result shows an inner confidence range of .928172 to .9482 for P_T values associated with S_q estimates. This uncertainty in the S_q location, reduces the validity in assuming that if lumping a PDF does not cause a substantial change in R , then the PDF will be adequate for computing high R values such as .96. Another more obvious example is the case where $n_2 = 6$ which shows an intervals of .835123 to .998 for $K = 3.5$ and .918483 to 1.0 when $K = 4.75$. The inner 98% ranges of S_q quantile values for $K = 4.75$ and $K = 3.5$ also show a substantial overlap. This case shows that even if the lumping process provides results showing small differences in R between $K = 3.5$ and 4.75 (using an unverified assumed known truncation point), the inference is meaningless. That is, the substantial uncertainty associated with computing R at unverified truncation points prevents making any assessment regarding the need for accurate representation of the extreme tail of the PDF in computing .96 R values.

These results are consistent with results of truncations of normal PDFs⁸ where, for truncations of less than 10 to 20 percent of the population, quantiles would fall within permissible limits of random variation, unless sample sizes are very large. Reference 5 shows various levels of uncertainty associated with computing high reliability from a stress-strength statistical model as a function of sample size. These results relate directly to the sample size issue discussed in this report.

The substantial sensitivities of R in each of the figures and tables relate to uncertainties in only one parameter, while the others are held constant. In design, the uncertainties in more than one parameter such as μ_α and CV could cause increased R sensitivity. There are many complex issues involved in obtaining a component population PDF for effective load severity scaling parameter, over lifetime. There is no industry standard approach to characterizing the load history and limited experience in determining loading PDFs. Therefore, the substantial influence on high reliability caused by loading PDF uncertainties could cause a serious problem in the implementation of a high reliability requirement.

These results are based on a single S-N curve, in contrast to the AHS round robin problem in which each participant used a different S-N curve. Thus, very substantial variability in the R-lifetime relationship can be expected even when the S-N curve shape and mean fatigue limit stress is fixed.

These results and the previous analyses of contaminated PDFs in Reference 5, support the concern expressed in Reference 4, for the issue of a decrease in reliability caused by degraded or non-conforming components. The approach of attempting to obtain statistically very high R values(.912) to compensate for uncertainties in assuming a PDF may not provide an effective margin of safety

or conservatism relative to a $.9_6$ requirement.

The comparisons between R_L and R_{UL} do not directly relate to PDF modeling for design. In the approach used in this report the lumped value in the PDF is made exactly equal to the extreme tail of a *known* PDF with which it is being compared. In the design process, the difference of interest is between a truncated assumed PDF and a "correct" PDF which is unknown. The lumping approach used in this study would tend to minimize the difference between R_L and R_{UL} relative to an actual design process.

No conclusion can be reached about an acceptable degree of truncation from this study. For λ_1 and $\lambda_2 \leq 3.5$ it appears that truncation is not acceptable for the $.9_6$ requirement. Variation in R from less than one "nine" to values approaching two "nines" were obtained for idealized conditions which minimize reliability differences as noted previously. For λ_1 and $\lambda_2 > 3.5$, the sampling results indicate that it does not appear to be feasible to obtain satisfactory representation of PDF unless very large data sets are available. More important, the issue of acceptable degree of truncation appears to be of secondary importance relative to the sensitivity of high R to the expected uncertainties in assuming a specific PDF representations.

CONCLUSIONS

Unstable high statistical reliability values for a fatigue loaded component can result from uncertainties in assuming the PDF model and determining its parameters without using very large data sets in the analysis.

Estimates of the extreme tail quantiles and their corresponding reliabilities can be unstable unless large data sets are used.

Analysis of the effects of extreme tail modification does not provide decisive information on the adequacy of PDF modeling. Tail modification effects on reliability are small relative to the effects of uncertainties in assuming a PDF model.

The primary conclusion, from the analytic evaluation in this report, is that computation of high statistical reliability may have little or no association with actual component reliability.

REFERENCES

1. Arden, R.W. and Immen, F.H., *U.S Army Requirements For Fatigue Integrity*, Proceedings of American Helicopter Society National Technical Specialists Meeting On Advanced Rotorcraft Structures, Williamsburg, VA, October 1990.
2. Everett, R.A., Bartlett, F.D., and Elber, W., *Probabilistic Fatigue Methodology For Six Nines Reliability*, AVSCOM Technical Report 90-B-009, NASA Technical Memorandum 102757, December 1990.
3. Schneider, G. and Gunsallus, C., *Continuation Of The AHS Round Robin On Fatigue and Damage Tolerance*, Presented At The American Helicopter Society Forty Seventh Annual Forum, Phoenix, AZ, May 1991.
4. Thompson, A.E and Adams, D.O. *A Computational Method For The Determination Of Structural Reliability Of Helicopter Dynamic Components*, Presented At The American Helicopter Society Annual Forum, Washington, D.C., May 1990.
5. Neal, D.M., Matthews, W.T. and Vangel, M.G., *Model Sensitivity In Stress-Strength Reliability Computations*, U.S. Army Materials Technology Laboratory, MTL TR 91-3, January 1991.
6. Neal, D.M., Matthews, W.T., Vangel, M.G. and Rudalevige, T., *A Sensitivity Analysis On Component Reliability From Fatigue Life Computations*, U.S. Army Materials Technology Laboratory MTL TR 92-5, February 1992.
7. Gunsallus, C., Memorandum To American Helicopter Society Fatigue And Damage Tolerance Subcommittee, August 28, 1991.
8. Hald, A., *Statistical Theory With Engineering Applications* Wiley, 1952, P. 146.

Table 1: Rainflow low-high load sequence derived from Felix-28

k	S_L	S_m	$n(k)$	k	S_L	S_m	$n(k)$
1	2.80	25.59	354	26	42.63	29.21	207
2	2.80	32.83	334	27	42.63	36.45	1274
3	6.42	29.21	416	28	46.25	21.97	274
4	10.04	29.21	609	29	46.25	25.59	6239
5	10.04	36.45	1228	30	46.25	29.21	4274
6	10.04	40.07	810	31	46.25	40.07	604
7	13.66	36.45	2	32	49.87	3.86	268
8	17.28	18.35	140	33	49.87	25.59	956
9	17.28	32.83	78	34	49.87	29.21	2179
10	20.91	32.83	2061	35	53.49	25.59	2
11	20.91	36.45	90	36	53.49	29.21	116
12	24.53	-7.00	140	37	57.12	25.59	5
13	24.53	18.35	140	38	57.12	29.21	185
14	24.53	36.45	2040	39	60.74	29.21	25
15	28.15	29.21	833	40	64.36	25.59	7
16	31.77	25.59	346	41	64.36	29.21	8
17	35.39	25.59	7904	42	64.36	32.83	75
18	35.39	29.21	56	43	67.98	29.21	9
19	35.39	32.83	71072	44	71.60	29.21	16
20	39.39	43.69	2529	45	75.22	25.59	7
21	39.01	21.97	3014	46	78.84	18.35	5
22	39.01	25.59	42825	47	78.84	25.59	1
23	39.01	29.21	6393	48	82.46	21.97	128
24	39.01	43.69	252	49	82.46	29.21	16
25	42.63	25.59	480	50	89.70	25.59	8

Table 2: Reliability from lumped and un-lumped PDFs as a function of the CVs

CVs	R_L	R_{UL}
0.05	> .976	.911
0.06	> .976	.97
0.07	.976	.96
0.08	.954	.9483
0.09	.9430	.93885
0.10	.93646	.93533

R_L - Reliability from lumping PDFs

R_{UL} - Reliability from normal PDFs

CVs - Coefficient of variations

$N_P = 80$ Passes, $\mu_\alpha = .70$ Load factor, $S_E = 54.5$ KSI Strength

Table 3: Effects of individual PDF contaminations on reliability estimates

μ_α	CV	N_P	R_U	R_{CL}	R_{CS}	R_{CLS}
.5	.07	80.0	> .912	.96	.93816	.93814
.7	.07	80.0	> .96	.93730	.93186	.928914
.7*	.07	80.0	> .976	.93733	.93224	.928955
.7	.10	4.0	> .96	.93848	.93092	.928940

* Both tails of PDFs are lumped at 3.5σ

R_U - Reliability uncontaminated PDFs

R_{CL} - Reliability contaminated(1%) load(α) PDF

R_{CS} - Reliability contaminated(1%) strength(S_E) PDF

R_{CLS} - Reliability from both load and strength PDFs contamination

Table 4: Reliability from lumped and unlumped PDFs VS. Load μ_α

μ_{alpha}	R_{UL}	R_L
0.4	$> .9_{12}$	$> .9_7$
0.5	$> .9_{12} [.999814]^*$	$.9_7 130$
0.6	$.9_{10}$	$.9_7 297$
0.7	$.9_6 [.998914]^*$	$.9_7 [.998955]^*$
0.8	$.999662$	$.999724$
0.9	$.984984$	$.984710$
1.0	$.855658$	$.851946$

R_L - Reliability from lumping PDFs

R_{UL} - Reliability from unlumped PDFs

* Results from contaminated PDFs

$N_P = 80$ Passes And CVs = .07

Table 5: Confidence interval on P_T and S_q quantile

N	Normal PDF $\mu = 100, CV = .10$					
	$K = 3.5$			$K = 4.75$		
	Median	Lower Bound	Upper Bound	Median	Lower Bound	Upper Bound
6	.999480* (67.07)**	.835123 (90.82)	.9 ₉ 78 (37.23)	.9 ₅ 58 (55.10)	.918483 (86.67)	1.00 (16.56)
10	.999669 (66.00)	.925734 (85.04)	.9 ₇ 86 (43.75)	.9 ₅ 81 (54.04)	.987086 (78.07)	.9 ₁₃ (24.78)
20	.999721 (65.48)	.981327 (78.92)	.9 ₆ 6 (50.64)	.9 ₅ 84 (53.36)	.998403 (70.56)	.9 ₁₀ 7 (34.27)
50	.999745 (65.36)	.995914 (73.92)	.9 ₅ 4 (56.13)	.9 ₅ 9 (52.81)	.999845 (63.95)	.9 ₈ 81 (41.14)
100	.999760 (65.13)	.998172 (71.05)	.9 ₄ 82 (59.01)	.9 ₅ 9 (52.68)	.9 ₄ 60 (60.52)	.9 ₈ (43.74)
1000	.999765 (65.02)	.999524 (66.96)	.999890 (63.07)	.9 ₈ (52.52)	.9 ₅ 6 (55.11)	.9 ₆ 7 (49.99)

* P_T Probability

** Corresponding S_q quantile value

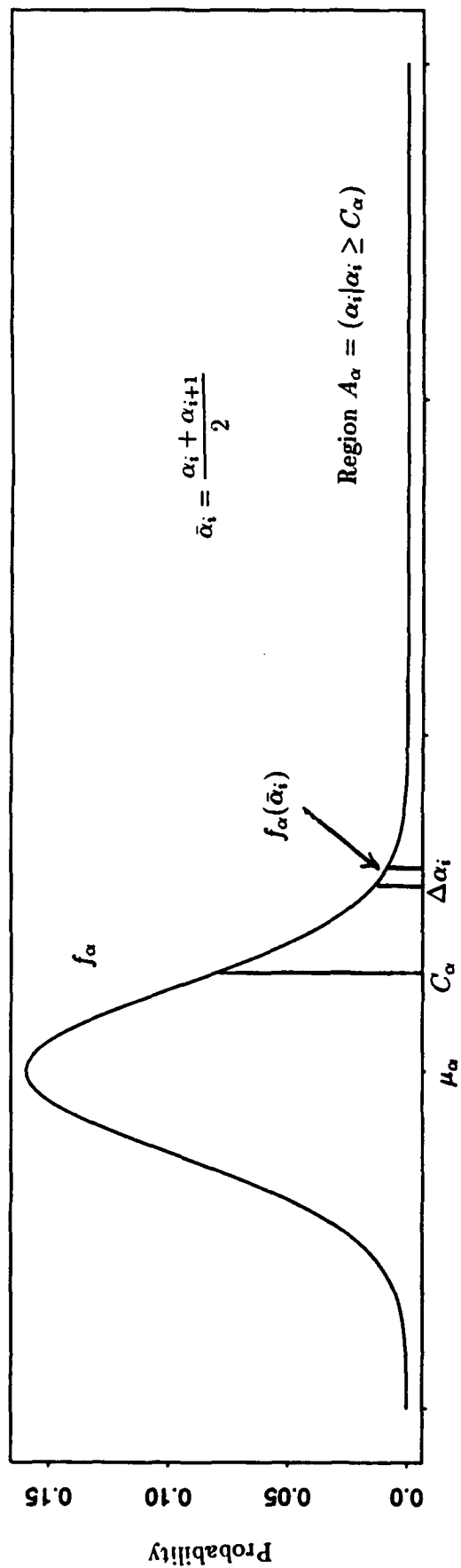


Figure 1a. Normal PDF for α load - JPF Region A_α

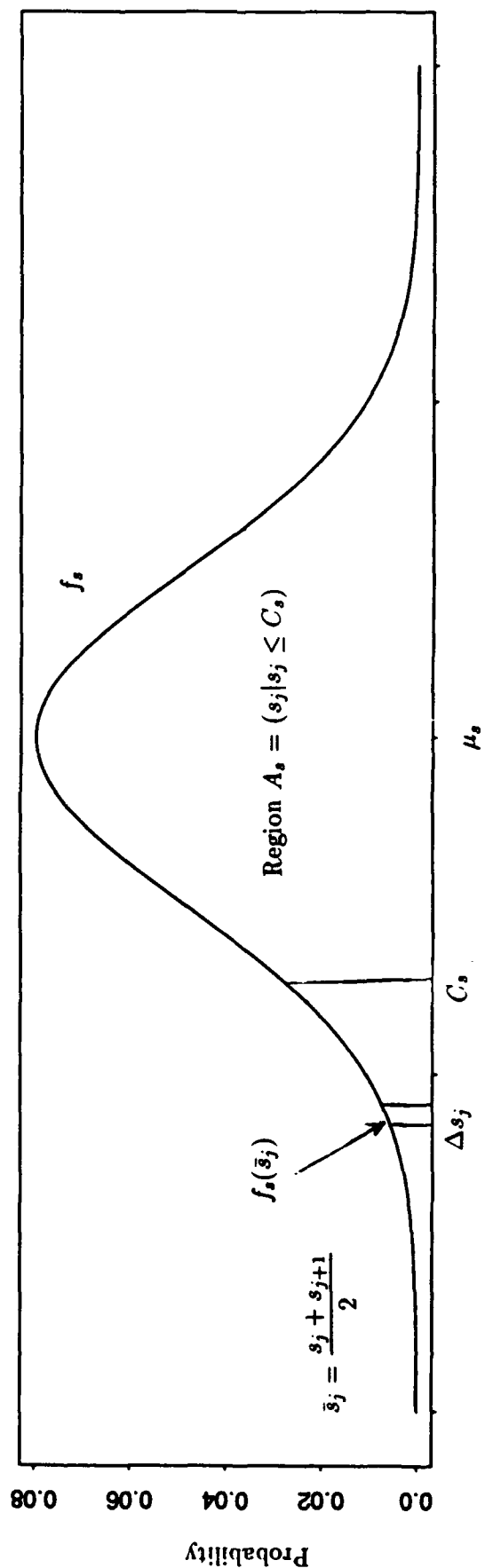


Figure 1b. Normal PDF for strength s and JPF Region A_s

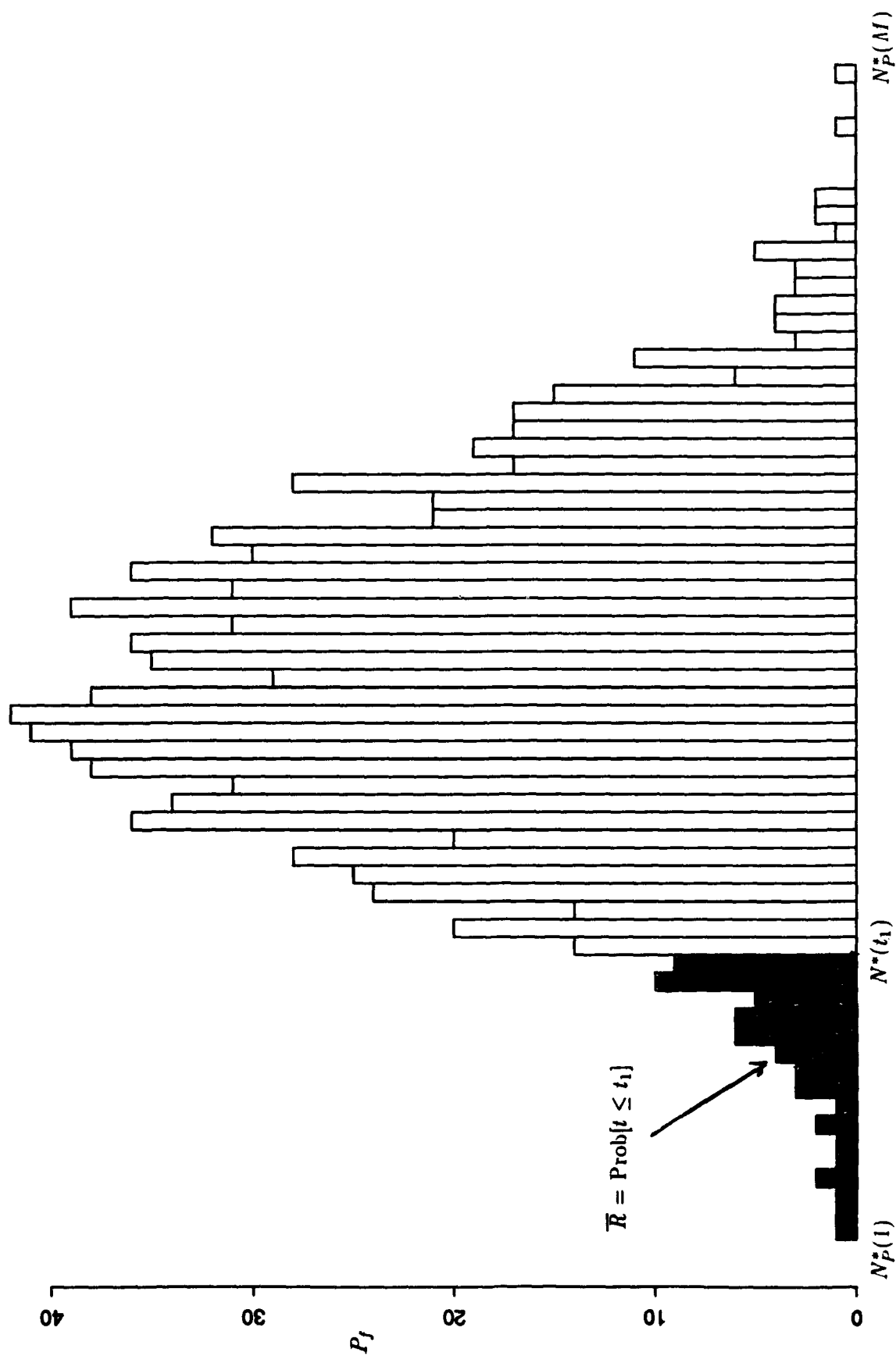


Figure 2. Discrete PDF for unreliability(\bar{R}) values.

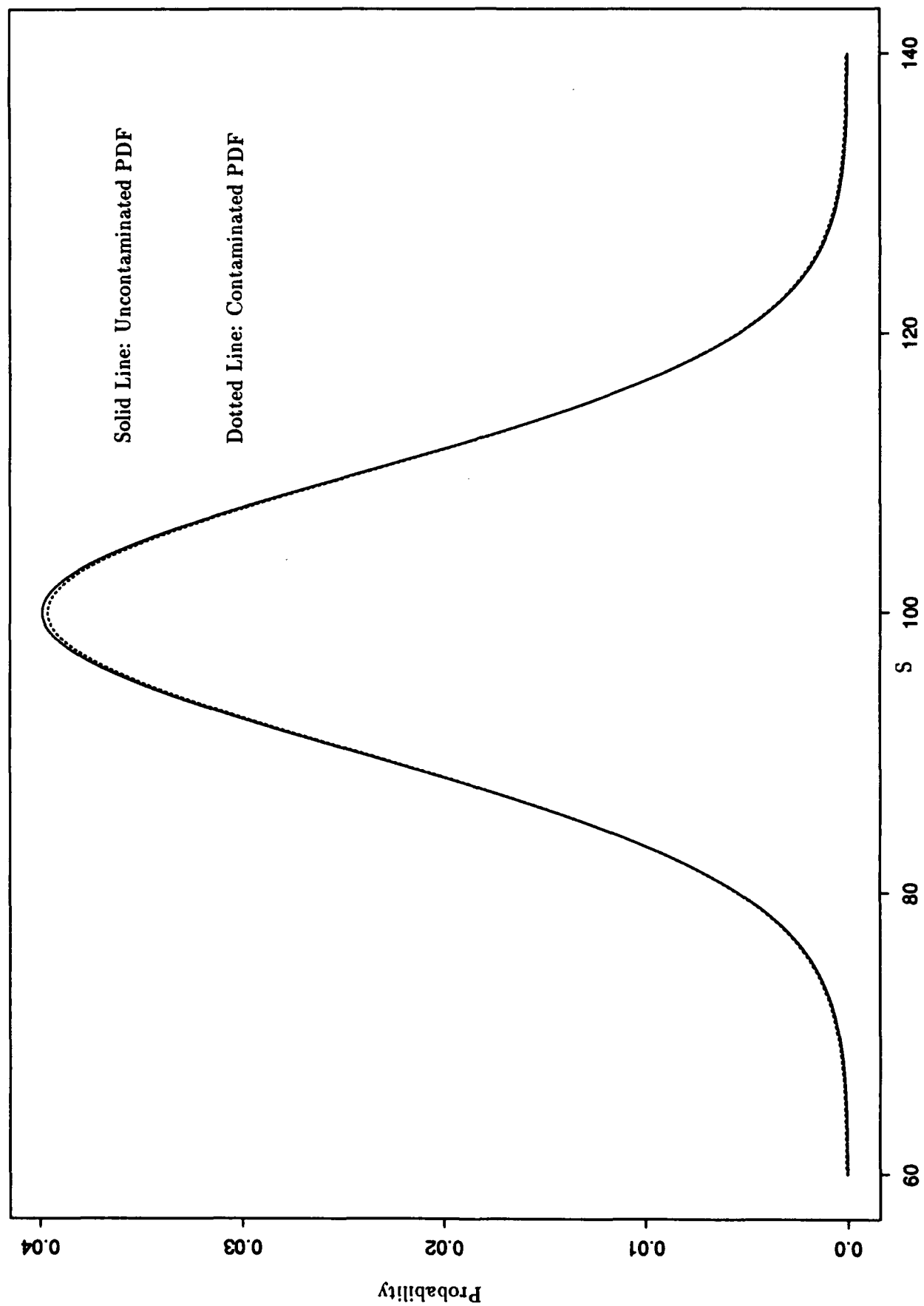


Figure 3. Contaminated(1%) and uncontaminated normal PDFs

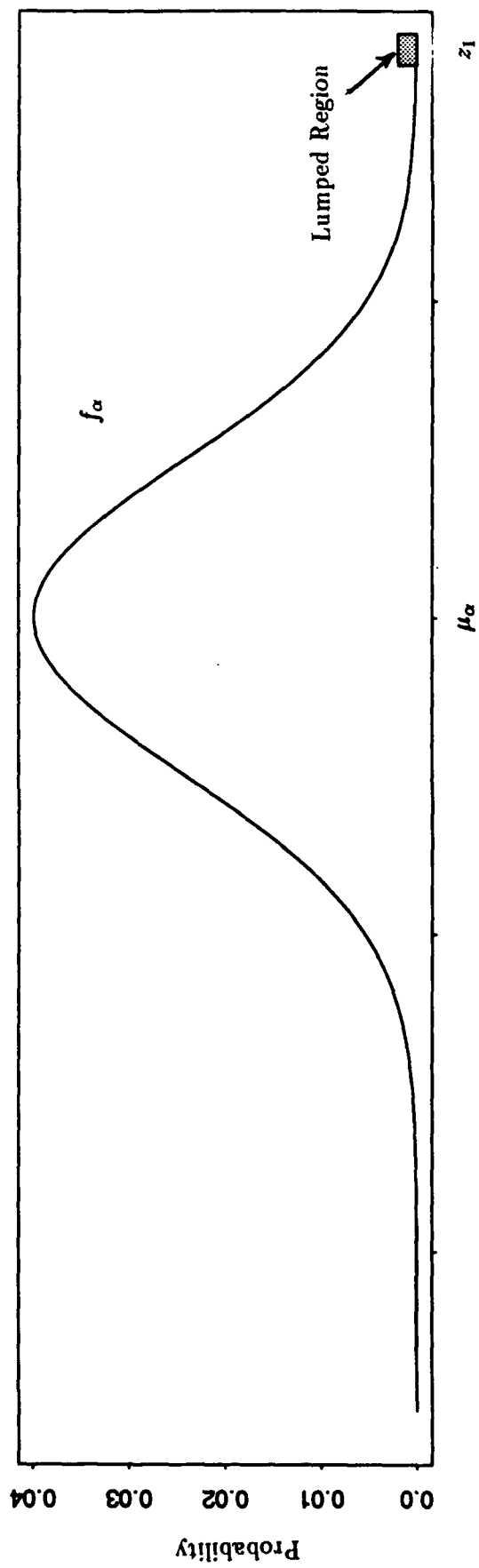


Figure 4a. Lumped normal load(α) PDF

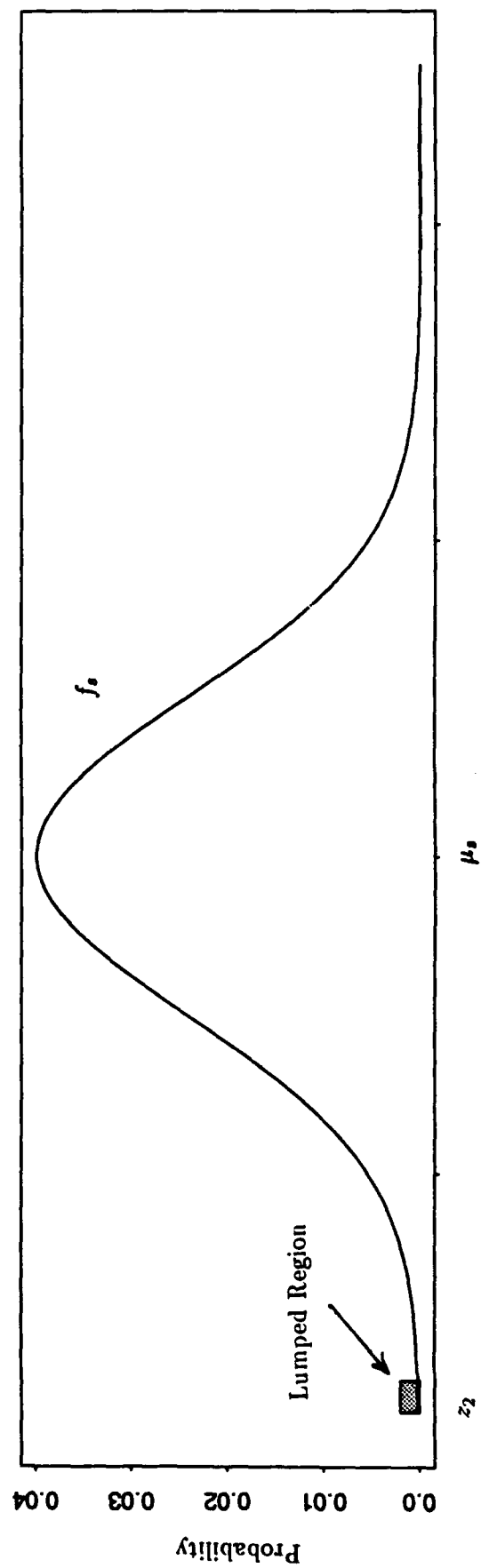


Figure 4b. Lumped normal strength(s) PDF

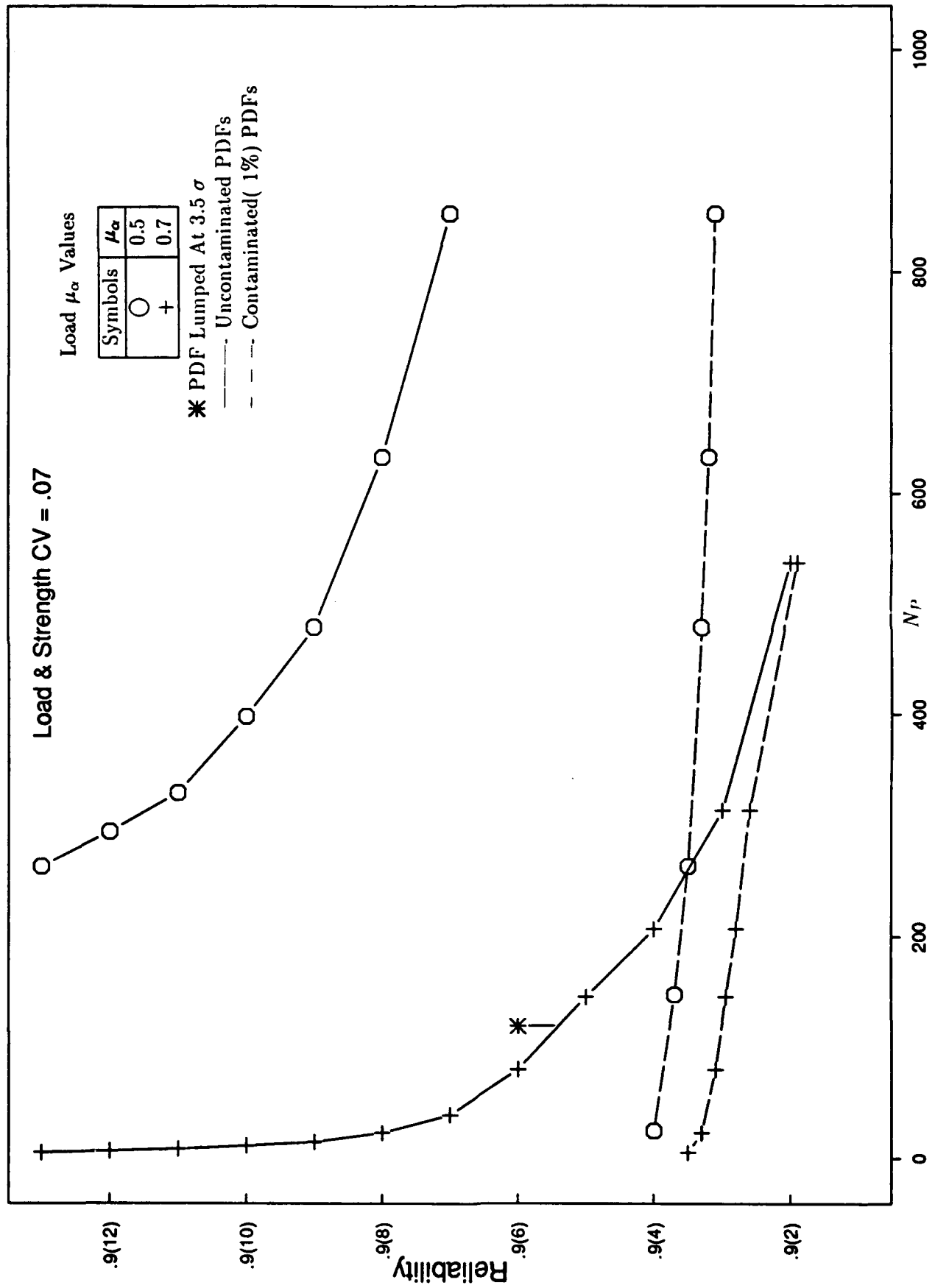


Figure 7. Reliability vs. N_p : Contaminated-Uncontaminated PDFs

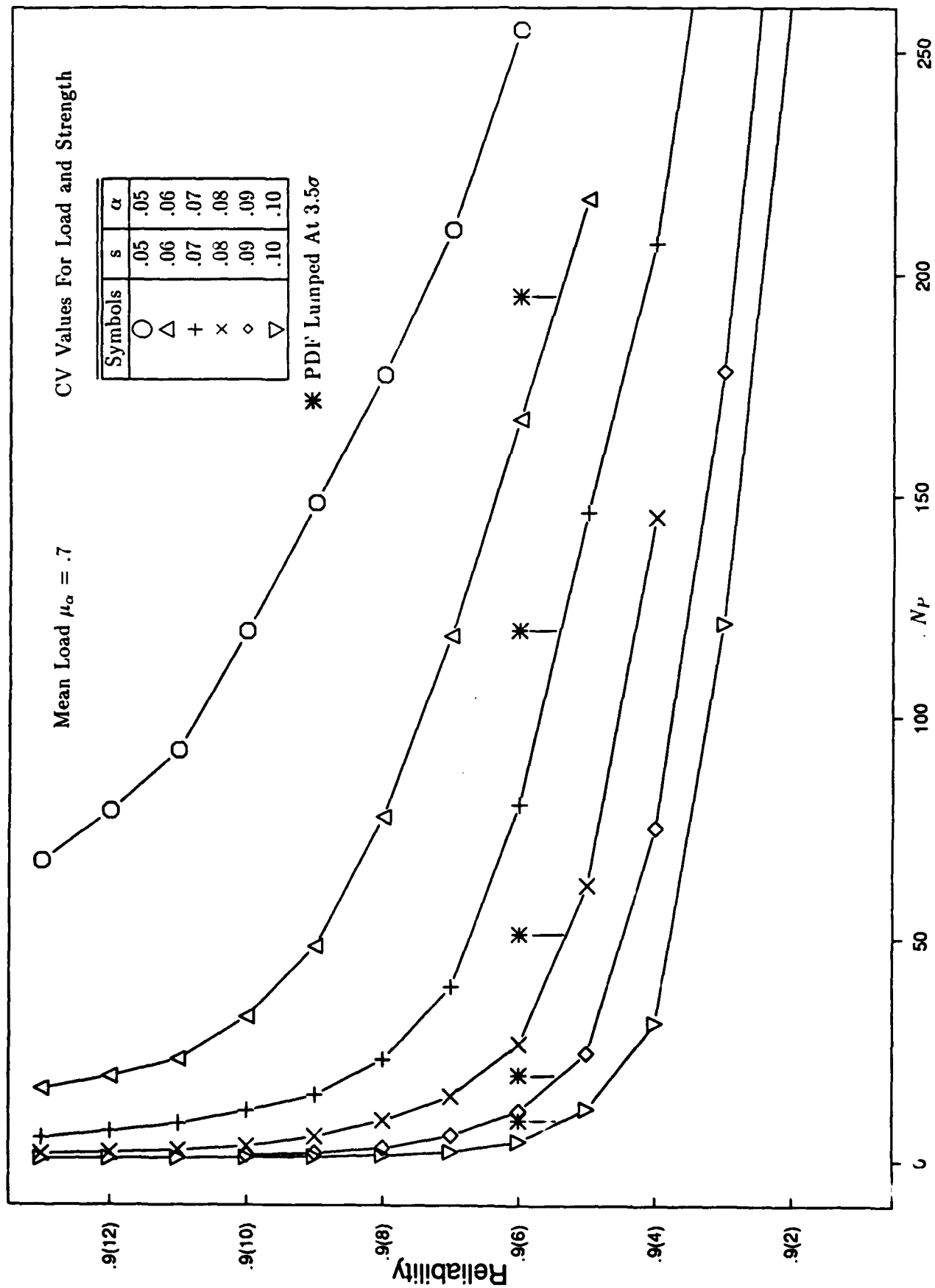


Figure 5. Reliability vs. N_p for specified CV values

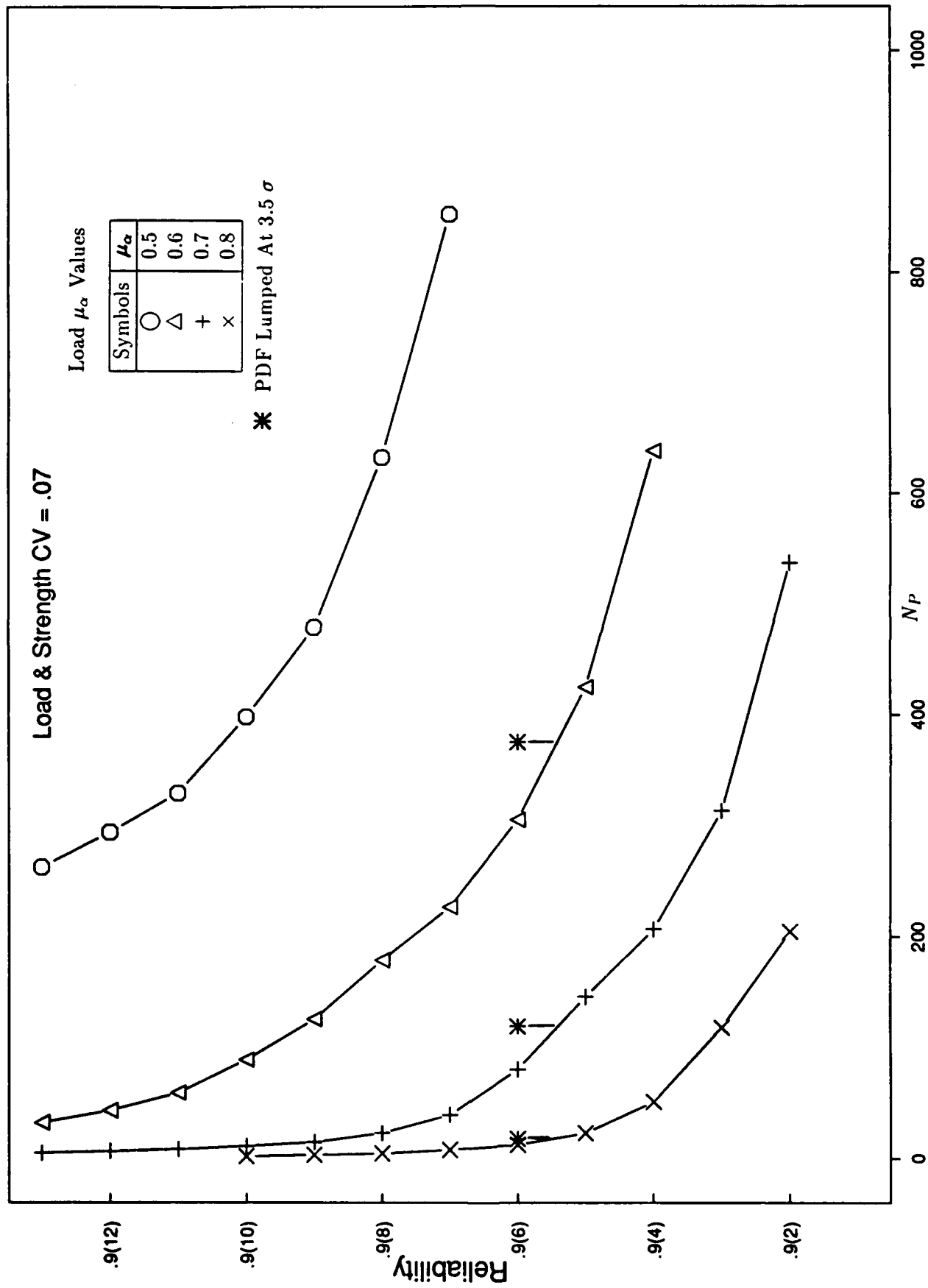


Figure 6. Reliability vs. N_p for specified μ_a values

DISTRIBUTION LIST

No. of Copies	To
1	Office of the Under Secretary of Defense for Research and Engineering, The Pentagon, Washington, DC 20301
1	Commander, U.S. Army Laboratory Command, 2800 Powder Mill Road, Adelphi, MD 20783-1145
1	ATTN: AMSLC-IM-TL
1	AMSLC-CT
2	Commander, Defense Technical Information Center, Cameron Station, Building 5, 5010 Duke Street, Alexandria, VA 22304-6145
1	ATTN: DTIC-FDAC
1	MIA/CINDAS, Purdue University, 2595 Yeager Road, West Lafayette, IN 47905
1	Commander, Army Research Office, P.O. Box 12211, Research Triangle Park, NC 27709-2211
1	ATTN: Information Processing Office
1	Commander, U.S. Army Materiel Command, 5001 Eisenhower Avenue, Alexandria, VA 22333
1	ATTN: AMCSCI
1	Commander, U.S. Army Materiel Systems Analysis Activity, Aberdeen Proving Ground, MD 21005
1	ATTN: AMXSYPMP, H. Cohen
1	Commander, U.S. Army Missile Command, Redstone Scientific Information Center, Redstone Arsenal, AL 35898-5241
1	ATTN: AMSMI-RD-CS-R/Doc
1	AMSMI-RLM
2	Commander, U.S. Army Armament, Munitions and Chemical Command, Dover, NJ 07801
1	ATTN: Technical Library
1	Commander, U.S. Army Natick Research, Development and Engineering Center, Natick, MA 01760-5010
1	ATTN: Technical Library
1	Commander, U.S. Army Satellite Communications Agency, Fort Monmouth, NJ 07703
1	ATTN: Technical Document Center
1	Commander, U.S. Army Tank-Automotive Command, Warren, MI 48397-5000
1	ATTN: AMSTA-ZSK
1	AMSTA-TSL, Technical Library
1	Commander, White Sands Missile Range, NM 88002
1	ATTN: STEWS-WS-VT
1	President, Airborne, Electronics and Special Warfare Board, Fort Bragg, NC 28307
1	ATTN: Library
1	Director, U.S. Army Ballistic Research Laboratory, Aberdeen Proving Ground, MD 21005
1	ATTN: SLCBR-TSB-S (STINFO)
1	Commander, Dugway Proving Ground, UT 84022
1	ATTN: Technical Library, Technical Information Division
1	Commander, Harry Diamond Laboratories, 2800 Powder Mill Road, Adelphi, MD 20783
1	ATTN: Technical Information Office
1	Director, Benet Weapons Laboratory, LCWSL, USA AMCCOM, Watervliet, NY 12189
1	ATTN: AMSMC-LCB-TL
1	AMSMC-LCB-R
1	AMSMC-LCB-RM
1	AMSMC-LCB-RP
3	Commander, U.S. Army Foreign Science and Technology Center, 220 7th Street, N.E., Charlottesville, VA 22901-5396
1	ATTN: AIFRTC, Applied Technologies Branch, Gerald Schlesinger
1	Commander, U.S. Army Aeromedical Research Unit, P.O. Box 577, Fort Rucker, AL 36360
1	ATTN: Technical Library

No. of Copies	To
1	Commander, U.S. Army Aviation Systems Command, Aviation Research and Technology Activity, Aviation Applied Technology Directorate, Fort Eustis, VA 23604-5577 ATTN: SAVDL-E-MOS
1	U.S. Army Aviation Training Library, Fort Rucker, AL 36360 ATTN: Building 5906-5907
1	Commander, U.S. Army Agency for Aviation Safety, Fort Rucker, AL 36362 ATTN: Technical Library
1	Commander, USACDC Air Defense Agency, Fort Bliss, TX 79916 ATTN: Technical Library
1	Commander, Clarke Engineer School Library, 3202 Nebraska Ave., N, Ft. Leonard Wood, MO 65473-5000 ATTN: Library
1	Commander, U.S. Army Engineer Waterways Experiment Station, P.O. Box 631, Vicksburg, MS 39180 ATTN: Research Center Library
1	Commandant, U.S. Army Quartermaster School, Fort Lee, VA 23801 ATTN: Quartermaster School Library
1	Naval Research Laboratory, Washington, DC 20375 ATTN: Code 5830
2	Dr. G. R. Yoder - Code 6384
1	Chief of Naval Research, Arlington, VA 22217 ATTN: Code 471
1	Edward J. Morrissey, WRDC/MLTE, Wright-Patterson Air Force Base, OH 45433-6523
1	Commander, U.S. Air Force Wright Research & Development Center, Wright-Patterson Air Force Base, OH 45433-6523 ATTN: WRDC/MLLP, M. Fomey, Jr.
1	WRDC/MLBC, Mr. Stanley Schulman
1	NASA - Marshall Space Flight Center, MSFC, AL 35812 ATTN: Mr. Paul Schuerer/EH01
1	U.S. Department of Commerce, National Institute of Standards and Technology, Gaithersburg, MD 20899 ATTN: Stephen M. Hsu, Chief, Ceramics Division, Institute for Materials Science and Engineering
1	Committee on Marine Structures, Marine Board, National Research Council, 2101 Constitution Avenue, N.W., Washington, DC 20418
1	Materials Sciences Corporation, Suite 250, 500 Office Center Drive, Fort Washington, PA 19034-3213
1	Charles Stark Draper Laboratory, 68 Albany Street, Cambridge, MA 02139
1	Wyman-Gordon Company, Worcester, MA 01601 ATTN: Technical Library
1	General Dynamics, Convair Aerospace Division P.O. Box 748, Fort Worth, TX 76101 ATTN: Mfg. Engineering Technical Library
1	Plastics Technical Evaluation Center, PLASTEC, ARDEC Bldg. 355N, Picatinny Arsenal, NJ 07806-5000 ATTN: Harry Peibly
1	Department of the Army, Aerostructures Directorate, MS-266, U.S. Army Aviation R&T Activity - AVSCOM, Langley Research Center, Hampton, VA 23665-5225
1	NASA - Langley Research Center, Hampton, VA 23665-5225
1	U.S. Army Propulsion Directorate, NASA Lewis Research Center, 2100 Brookpark Road, Cleveland, OH 44135-3191
1	NASA - Lewis Research Center, 2100 Brookpark Road, Cleveland, OH 44135-3191
2	Director, U.S. Army Materials Technology Laboratory, Watertown, MA 02172-0001 ATTN: SLCMT-TML
2	Authors

<p>U.S. Army Materials Technology Laboratory Watertown, Massachusetts 02172-0001 ASSESSMENT OF HELICOPTER COMPONENT STATISTICAL RELIABILITY COMPUTATIONS - WILLIAM T. MATTHEWS and DONALD M. NEAL Technical Report MTL TR 92-71, September 1992. 24 pp - illustrations, tables</p>	<p>AD</p> <p>UNCLASSIFIED UNLIMITED DISTRIBUTION</p> <p>Key Words Reliability Fatigue life Flight loads</p>	<p>U.S. Army Materials Technology Laboratory Watertown, Massachusetts 02172-0001 ASSESSMENT OF HELICOPTER COMPONENT STATISTICAL RELIABILITY COMPUTATIONS - WILLIAM T. MATTHEWS and DONALD M. NEAL Technical Report MTL TR 92-71, September 1992. 24 pp - illustrations, tables</p>	<p>AD</p> <p>UNCLASSIFIED UNLIMITED DISTRIBUTION</p> <p>Key Words Reliability Fatigue life Flight loads</p>
<p>This report identifies potential errors in computing high statistical reliability for a required component fatigue life. The reliability values were determined from application of a joint probability density (JPD) analysis used in an American Helicopter Society round robin safe life problem. In the analysis normal probability density functions (PDFs) were assumed for both the material strength and the spectrum load values. The PDF model parameters were varied and the PDFs were slightly modified (contaminated) in order to examine the sensitivity in computing high statistical reliability when uncertainties exist in assuming the PDF. Lower tails of the PDFs were also modified by truncation, independent of the model contamination, in order to determine the relative influence on reliability from tail modifications as compared with the parameter uncertainties and contamination. The stability of statistical estimates of the extreme tail quantiles and their corresponding probabilities as a function of sample size were examined for a generic distribution. Assuming a PDF to represent load or material strength is a substantially more critical issue than accurate representation of the extreme lower tail of the PDF when computing high reliability. Sampling trials for extreme tail quantiles and reliabilities indicate that unstable values can result from sample sizes of 100. The primary conclusion from these analytic results is that the computation of a high statistical reliability may have little or no association with actual engineering high reliability.</p>	<p>This report identifies potential errors in computing high statistical reliability for a required component fatigue life. The reliability values were determined from application of a joint probability density (JPD) analysis used in an American Helicopter Society round robin safe life problem. In the analysis normal probability density functions (PDFs) were assumed for both the material strength and the spectrum load values. The PDF model parameters were varied and the PDFs were slightly modified (contaminated) in order to examine the sensitivity in computing high statistical reliability when uncertainties exist in assuming the PDF. Lower tails of the PDFs were also modified by truncation, independent of the model contamination, in order to determine the relative influence on reliability from tail modifications as compared with the parameter uncertainties and contamination. The stability of statistical estimates of the extreme tail quantiles and their corresponding probabilities as a function of sample size were examined for a generic distribution. Assuming a PDF to represent load or material strength is a substantially more critical issue than accurate representation of the extreme lower tail of the PDF when computing high reliability. Sampling trials for extreme tail quantiles and reliabilities indicate that unstable values can result from sample sizes of 100. The primary conclusion from these analytic results is that the computation of a high statistical reliability may have little or no association with actual engineering high reliability.</p>	<p>This report identifies potential errors in computing high statistical reliability for a required component fatigue life. The reliability values were determined from application of a joint probability density (JPD) analysis used in an American Helicopter Society round robin safe life problem. In the analysis normal probability density functions (PDFs) were assumed for both the material strength and the spectrum load values. The PDF model parameters were varied and the PDFs were slightly modified (contaminated) in order to examine the sensitivity in computing high statistical reliability when uncertainties exist in assuming the PDF. Lower tails of the PDFs were also modified by truncation, independent of the model contamination, in order to determine the relative influence on reliability from tail modifications as compared with the parameter uncertainties and contamination. The stability of statistical estimates of the extreme tail quantiles and their corresponding probabilities as a function of sample size were examined for a generic distribution. Assuming a PDF to represent load or material strength is a substantially more critical issue than accurate representation of the extreme lower tail of the PDF when computing high reliability. Sampling trials for extreme tail quantiles and reliabilities indicate that unstable values can result from sample sizes of 100. The primary conclusion from these analytic results is that the computation of a high statistical reliability may have little or no association with actual engineering high reliability.</p>	<p>This report identifies potential errors in computing high statistical reliability for a required component fatigue life. The reliability values were determined from application of a joint probability density (JPD) analysis used in an American Helicopter Society round robin safe life problem. In the analysis normal probability density functions (PDFs) were assumed for both the material strength and the spectrum load values. The PDF model parameters were varied and the PDFs were slightly modified (contaminated) in order to examine the sensitivity in computing high statistical reliability when uncertainties exist in assuming the PDF. Lower tails of the PDFs were also modified by truncation, independent of the model contamination, in order to determine the relative influence on reliability from tail modifications as compared with the parameter uncertainties and contamination. The stability of statistical estimates of the extreme tail quantiles and their corresponding probabilities as a function of sample size were examined for a generic distribution. Assuming a PDF to represent load or material strength is a substantially more critical issue than accurate representation of the extreme lower tail of the PDF when computing high reliability. Sampling trials for extreme tail quantiles and reliabilities indicate that unstable values can result from sample sizes of 100. The primary conclusion from these analytic results is that the computation of a high statistical reliability may have little or no association with actual engineering high reliability.</p>